Chapter 2
Medicine and Engineering Related Researches on the Utility of Two Dimensional Nuchal Translucency

Abstract A thorough literature review on current research for trisomy 21 detection using ultrasound will be carried out for existing modality's drawback investigation. Due to its critical restriction, computing on ultrasound markers in term of its recognition, segmentation and measurement are essentially required. 3D reconstruction of nuchal translucency becomes a breakthrough to select the appropriate scanning plane of ultrasound markers. It shall resolve the problematic issue on scanning plane selections which depends on operator assumption and experience. Data sources from hospital patient scanning should obtain the approval from Medicine ethical committee. Consent and simple agreement document shall be prepared. The main ultrasound images sources will be taken from Health Center Universiti Teknologi Malaysia, Hospital Universiti Sains Malaysia, and Hospital Universiti Kebangsaan Malaysia. External collaboration parties are Hospital Sultanah Aminah and Technische Universitat Ilmenau, Germany. Other than fetal data, maternal health data will also be recorded. This data is important to obtain the knowledge of correlation between fetal and mother data. It is recommended that pregnant women should be older than 30 years old. This chapter will describe the book in terms of its background, history and the related works in greater detail. The focus will be on the Trisomy 21 background, history, existing detection techniques, and ultrasound application using 2D and 3D image formation on fetal abnormalities detection. Previous related research works are discussed and each of their limitation is remarked.

2.1 Review of Trisomy 21

Trisomy 21 or Down syndrome is the most common disease of chromosomal abnormalities, where the patients' cells have extra copy of 21st chromosomes as compared to normal paired chromosomes, leading to abnormal structure and function of many organs, including mental retardation, congenital heart disease, and intestinal plugs. Other examples of Trisomy include Trisomy 18 and Trisomy 13. Trisomy 18 or Trisomy 13 simply means there are three copies of the 18th chromosome (or of the 13th chromosome) present in each cell of the body, rather than the usual pair. It was firstly reported by Down in 1866 and it is named after him as Down syndrome (Down

K. W. Lai and E. Supriyanto, *Detection of Fetal Abnormalities Based on Three Dimensional Nuchal Translucency*, SpringerBriefs in Applied Sciences and Technology,
DOI: 10.1007/978-981-4021-96-8_2, © The Author(s) 2013

1995). The main characteristics of this syndrome are severe mental retardation, with a unique facial and body deformities (Wee et al. 2010a, b).

The birthrate of Down's syndrome is approximately one in every 800–1000 live births. Affected babies are likely to suffer from severe mental and physical disabilities, affecting in particular the heart, gastrointestinal tract, eyes and ears. Down's syndrome generally lives to adulthood, but they need to receive long-term caregivers. In actual life, patient with trisomy 21 requires lifelong care and supports from their families, which will definitely cause heavy burden in both mental and economic wise.

2.2 History of Trisomy 21 Detection

In 1930s, Waardenburg and Bleyer were the first persons to speculate that the cause of Trisomy 21 might be due to chromosomal abnormalities. With the discovery of karyotype techniques in the 1950s, it became possible to identify abnormalities of chromosomal number or shape. In 1959, Jerome and Patricia were the first to determine the cause of Trisomy was due to the triplication of 21st chromosome. The chromosomes are thread-like structures composed of DNA and other proteins. They are present in every body cell and carry the genetic information needed for cell development. Genes, which are units of information, are encoded in the DNA. Normally, human cells have 46 chromosomes which can be arranged in 23 pairs. Of these 23, 22 are alike in males and females; these are called the autosomes. The 23rd pair is the sex chromosomes ('X' and 'Y'). Each member of a pair of chromosomes carries the same information, in that the same genes are in the same spot on the chromosome. However, variations of that gene may be present. For example, the genetic information for eye color is a "gene;" the variations for blue, green, etc.

Divisions of human cells are separated into two different ways. The first is ordinary cell division, which is also known as mitosis, by which the body grows. In this method, one cell becomes two cells which have the exact same number and type of chromosomes as the parent cell. The second method of cell division occurs in the ovaries and testicles, which is known as meiosis consisting of one cell splitting into two, with the resulting cells having half the number of chromosomes of the parent cell. So, normal eggs and sperm cells only have 23 chromosomes instead of 46. Figure 2.1 below shows the normal 23 pairs of chromosomal arrangement.

In Down syndrome, 95 % of all cases are caused by this event, where one cell has two 21st chromosomes instead of one, so the resulting fertilized egg has three 21st chromosomes. Hence the scientific name, Trisomy 21. Figure 2.2 below illustrate the structure of abnormal chromosomal arrangement.

The cause of trisomy 21 with an extra copy of chromosome is still unknown, but early researches have proved that it is highly associated with the maternal ages. Unfortunately, there are no effective prevention and treatment measures for this disease.

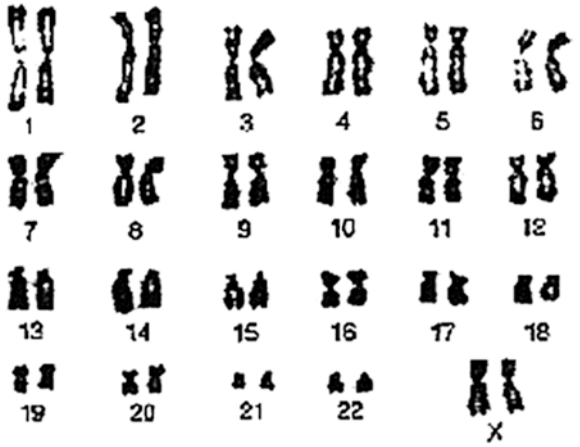

Fig. 2.1 Normal pairs of human chromosomal arrangement (Leshin 1997)

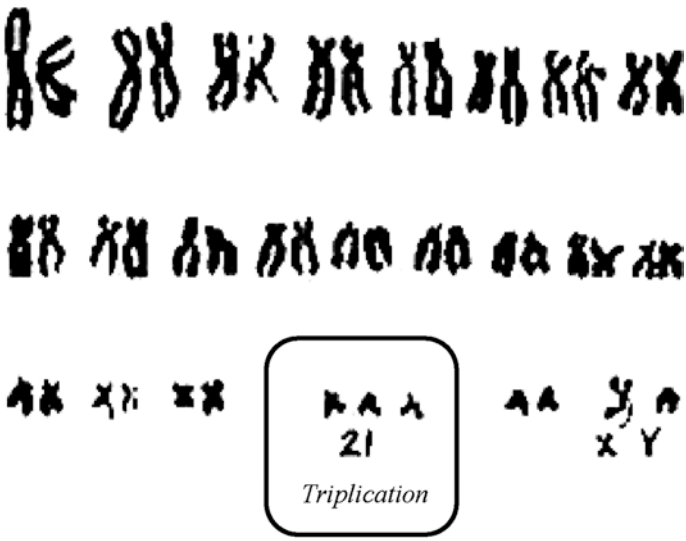

Fig. 2.2 Structure of abnormal chromosomal arrangement. *Note* XY means this is a karyotype of male with trisomy 21 (Leshin 1997)

2.3 Maternal Age Factor

Maternal age is the best known risk factor for trisomy 21 and other chromosomal abnormalities since 1980. The reasons why the age of the mother increases the risk for chromosomal abnormalities are still unknown currently. However, one of idea that is predicted by scientists is that older eggs are more prone to nondisjunction

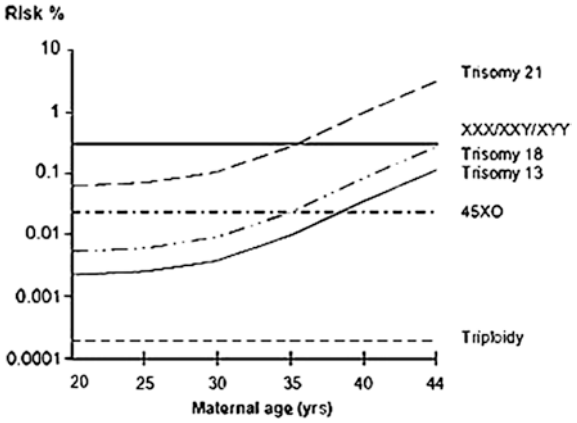

Fig. 2.3 Maternal age-related risk for chromosomes abnormalities (*sources* FMF)

which in turn leads to the occurrence of trisomy 21, 18 and 13. For example, female eggs ovulated at age 40 have been in meiosis I for more than 40 years. During this time, events in the cell or environmental agents might damage the egg, making nondisjunction more likely.

Based on Huether (1998), maternal age highly influences the risk of conceiving Trisomy 21 baby. The statistics show that at maternal age in between 20 and 24, the probability is one in 1562; it increases dramatically to one in 214 at maternal age from 35 up to 39, and the probability for maternal with age 45 above is one in 19. The data shows the fact that elder maternal age has higher probability of conceiving Trisomy 21 baby.

The risk of Trisomy 21 and some other chromosomal abnormalities in an unborn child is known to increase with the age of the mother and it is this knowledge which forms the basis for selection of pregnant women for further investigation. Figure 2.3 shows the example of maternal age-related risk for chromosomes abnormalities. It can be observed that the increase of maternal age will have positive exponential risk increment of trisomy 21.

2.4 Effect of Previous Pregnancies Factor

Normally, couples who have one child with trisomies have a slightly increased risk of having a second child with trisomies. The recurrent risk of trisomies increase in current pregnancy because some couple with a previously affected pregnancy have parental mosaicism or a genetic defect that interferes with the normal process of disjunction (Snijders et al. 1999). In woman who had a previous pregnancy with trisomies, the risk of recurrent in the subsequent pregnancy is 0.75 % higher than maternal and gestational age-related risk for trisomies at the time of testing.

2.5 Existing Detection Methods of Trisomy 21

Basically, there are three different methods for Trisomy 21 detection during first and second trimester of pregnancy, including specific B-mode ultrasound marker assessment, maternal serum marker assessment and genetic examination of amniotic fluid or fetus blood. Brief description of each existing detection method in clinical practice are discussed as per below and comparisons of their pro and cons were conducted.

2.5.1 Ultrasound

There is extensive evidence (Nicolaides et al. 1992) that effective prenatal screening for major chromosomal abnormalities can be provided in the first trimester of pregnancy. Ultrasound screening in first trimester of pregnancy provides an effective way of screening chromosomal abnormalities (aneuploidy). Recent studies shows that assessment of particular ultrasound markers offer promising noninvasive method for fetal abnormalities detection, such as nuchal translucency, nasal bone, long bone biometry, maxillary length, cardiac echogenic focus and ductus venous (Nicolaides et al. 1999). American college of obstetricians and gynecologists has updated their guidelines and has recommended that all the pregnant women should be counseled about availability of screening tests for fetal aneuploidies (Acog 2007). By determining the risk in first trimester earlier reassurance for those with normal babies and safer termination for those with aneuploidy fetuses, is possible.

Medical literature has proven a fetus with congenital disease such as Trisomy 21, heart disease and bone disease will have thicker transparent layer of subcutaneous fetal neck or called Nuchal Translucency. The term Nuchal Translucency was termed by Nicolaides, pioneer in prenatal Trisomy 21 early assessment at Fetal Medicine Foundation (FMF), UK (Nicolaides et al. 1992). The formation of this transparent layer of skin was due to blockage of blood or lymphatic circulation, resulting in accumulation of liquid behind fetus's neck (Souka et al. 2001; Hyett et al. 1995; Kagan et al. 2009; Snijders et al. 1998). Single marker evaluation of NT can help doctors to evaluate the chances of fetal with Down syndrome up to 70 % (Abuhamad 2005; Zosmer et al. 1999). Some previous publication (Kagan et al. 2008; Cicero et al. 2003) used to assess the risk of Trisomy 21 during early pregnancy using NT measurement combining with pregnancy-induced plasma protein A (PAPP A) and free-Beta human chorionic gonadotropin (free ß-hCG), is able to drive the rate up to 90 % (one-stop reference trimester Down syndrome screening). Figure 2.4 shows the clinical anatomy of nuchal translucency formation.

With respect to the NT structure shown above, it can be examined using B-mode ultrasonic imaging by adhered to FMF guideline, as shown in Fig. 2.5 in

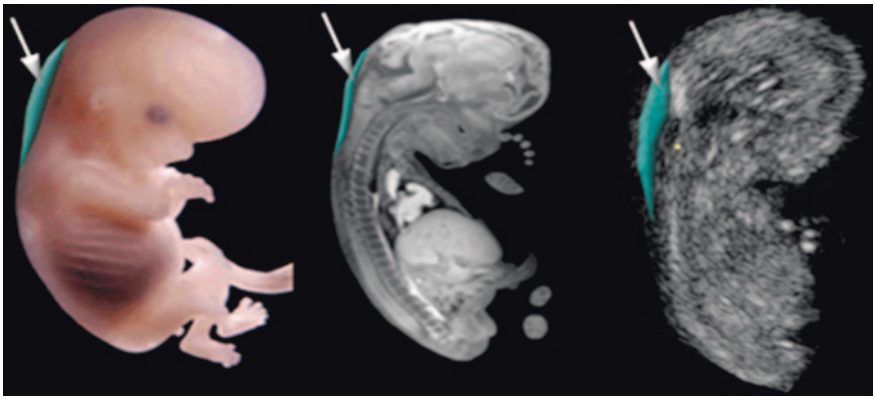

Fig. 2.4 Formation of nuchal translucency thicknesses due to fluid accumulation behind fetus' neck

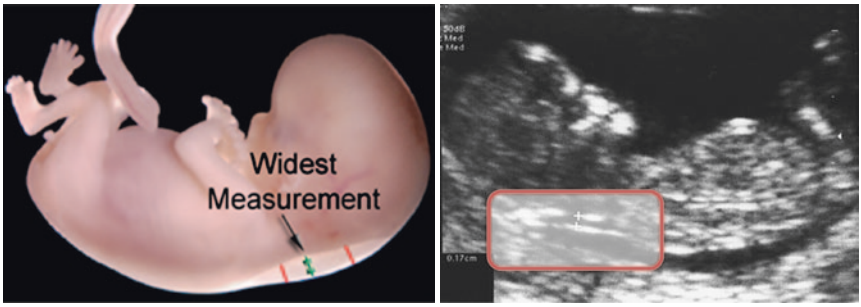

Fig. 2.5 Nuchal translucency thickness measurements for Trisomy 21 assessment during first trimester pregnancy

sagittal mode. NT thickness should be measured during the specific gestation ages, from 11 until 13 weeks plus 6 days, within Crump Rump Length (CRL) measured in between 45 and 84 mm. Only the maximum thickness of fold thickness regards as final measurement for Trisomy 21 assessment. Note that higher thickness of NT layer indicates the higher probability of Trisomy 21.

Maximum NT thickness measurement using B-mode ultrasonic imaging should strictly adhere to a tedious protocol developed by FMF. Although it provides a noninvasive method for Trisomy 21 assessment, there are some critical weaknesses of existing manual 2D marker measurement method, as discussed in Sect. 1.2. Details of medicine and technical engineering literature for ultrasound marker assessment are discussed in Sect. 2.7.1.

2.5.2 Maternal Serum Markers

Maternal serum markers are defined as a hormone or protein found in maternal blood that can serve as a sign of abnormality. The most common of these markers being alpha fetoprotein (AFP), pregnancy associated plasma proteins A (PAPP-A), unconjugated oestriol (uE3), free ß-human chorionic gonadotrophin (free ß-hCG) and inhibin A (DIA). It has been recognized that the chromosomally abnormal pregnancy is associated with the abnormal level of maternal serum markers. Both AFP and UE3 are produced by fetus while DIA, PAPP-A and free ß-hCG are produced by placental trophoblast during pregnancy (Wald et al. 1996).

In the first trimester, the PAPP-A level is, on average, low in Down's syndrome pregnancies (about half that of unaffected pregnancies) (Wald et al. 1996). In the second trimester AFP and uE3 levels are, on average, low (about three-quarters that of unaffected pregnancies) and inhibin- A and free ß-hCG levels are, on average, high (about double that of unaffected pregnancies). Kagan et al. (2008) had demonstrated that the maternal serum markers screening for calculation of accurate patient-specific risks for trisomy 21 is essential to take into account gestation age, maternal weight, ethnicity, smoking status and method of conception.

Before these biochemistry screening methods were introduced in the late 1980s, maternal ages are the single evaluation factor with the aim to select the 'high-risk' group of Trisomy 21. At 16 weeks of gestation, AFP, uE3 and hCG in Trisomy 21 pregnancies are sufficiently different from normal pregnancies to distinguish the risk group. This method improved the effectiveness than maternal age alone, identified about 50 until 70 % of the fetuses with Trisomy 21. After the emergence of ultrasonic marker NT in 1992 by Nicholaides et al. screening by a combination of maternal age and fetal NT thickness at 11–13 + 6 weeks of gestation was introduced. This method has now been shown to identify about 75 % of affected fetuses for a screen-positive rate of about 5 %. Subsequently, maternal age was combined with fetal NT and maternal serum biochemistry (free ß-hCG and PAPP-A) in the first-trimester to identify about 85–90 % of affected fetuses.

2.5.3 Genetic Testing

Basically, genetic testing considering amniocentesis and chorionic villus sampling (CVS), the process of extracting amniotic fluid for analysis to determine the presence of genetic defects during pregnancy. This method is a confirmatory testing for chromosomal abnormalities detection which provides high accuracy as compared to previous described two methods. Amniocentesis is usually performed between 15 and 22 post-menstrual weeks of pregnancy. For earlier genetic

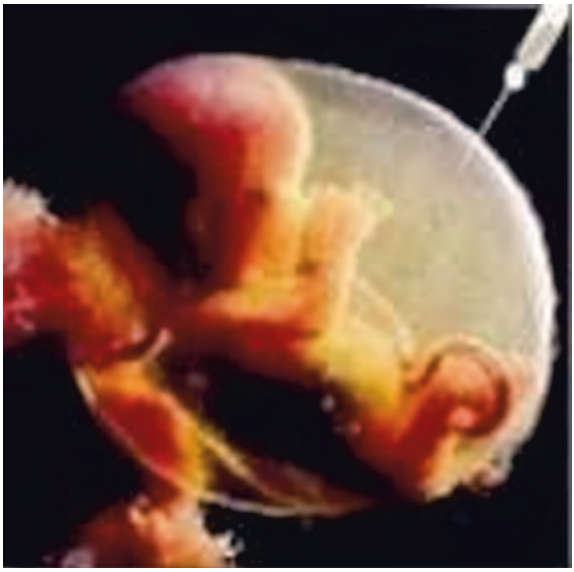

Fig. 2.6 Amniotic fluid extraction using needle with ultrasound guidance

testing, CVS act as an alternative to the second trimester amniocentesis and can be performed from 10 weeks gestation age onwards. The procedure includes ultrasound guidance of a thin needle inserted through the abdominal wall to withdraw 2 tablespoons of amniotic fluid for analysis. Figure 2.6 illustrates the process of amniocentesis.

The risk for complications or miscarriage from having an amniocentesis performed is about 1 out of every 200 women, or 0.5 %. Complications include vaginal spotting or bleeding, leakage of amniotic fluid, severe cramping, fever, or infection. Meanwhile the risk of CVS during first trimester pregnancies is 1 in 100 women, or 1 %. According to FMF report, amniocentesis is also possible at 10 until 14 weeks of gestation. However, randomized studies have demonstrated that after early amniocentesis the rate of fetal loss is about 2 % higher (3 in 100 women).

2.5.4 Summary

Based on the literatures and consultation of collaborator hospital in Malaysia, we have summarized three different methods of Trisomy 21 detection, as shown in Table 2.1. Since genetic testing involves invasive examination with at least fetal loss probability of 1 in 100 women, if the fetuses have low chances of being Trisomies 21 babies, it is not recommended for pregnant women to perform these invasive examinations. Among the methods abovementioned, ultrasound prenatal screening for Trisomy 21 detection is the most favorable due to its intuitive,

Table 2.1 Method comparisons summary

Methods	**Markers**	Invasiveness	Gestation age	Risk (%)	Cost[a] (RM)	Operation durations	Recovery durations	Results availability
Ultrasound	Nuchal translucency, Nasal bone	non-invasive	1st Trimester	low	25	30 min	none	real time
Maternal serum markers	PAPP-A, free ß-hCG, AFP	non-invasive	1st/2nd Trimester	low	350	<5 min	negligible	3 days
Genetic testing	Amniotic fluid, Chorionic villus	invasive	2nd Trimester	min 1–2 %	400 (QF-PCR) 580 (Karyotyping)	30 min	1 day	2 weeks

[a]Costs shown is applied on public hospital, it might be different at private or specialist hospital in Malaysia
[b]Quantitative fluorescent polymerase chain reaction (QF-PCR) is an alternative and rapid diagnostics method compare to full karyotyping

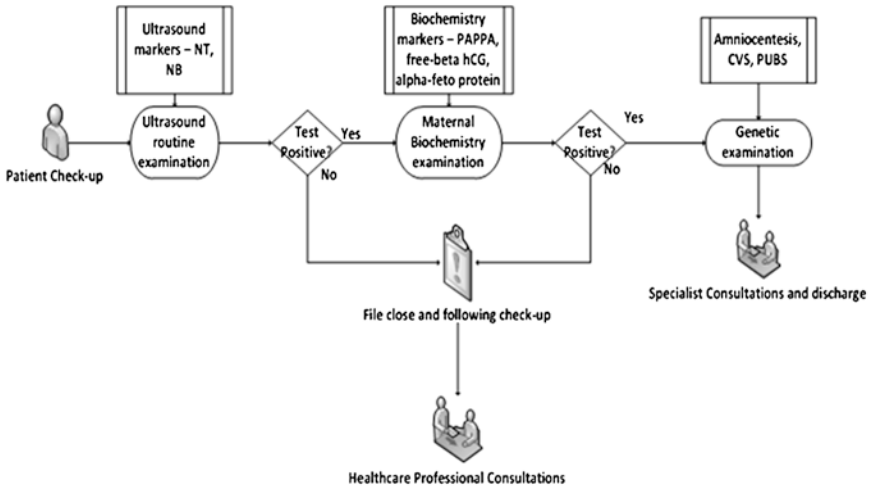

Fig. 2.7 Clinical work flow for Trisomy 21 detection process

Table 2.2 Detection rates for Trisomy 21 using single and hybrid combination methods

Methods	DR (%)
Maternal age (MA)	30
MA and maternal serum biochemistry at 15–18 weeks	50–70
MA and fetal nuchal translucency (NT) at 11–13 + 6 weeks	70–80
MA and fetal NT and maternal serum free b-hCG and PAPP-A at 11–13 + 6 weeks	85–90
MA and fetal NT and fetal nasal bone (NB) at 11–13 + 6 weeks	90
MA and fetal NT and NB and maternal serum free b-hCG and PAPP-A at 11–13 + 6 weeks	95
Amniocentesis or CVS	>99

non-invasiveness, flexibility, low risk, performance cost and time effectiveness. Figure 2.7 shows the process of clinical practices for chromosomal abnormalities detection, and Table 2.2 explained the detection rates of Trisomy 21 using each and hybrid combination methods.

With the aim of early detection in first trimester of pregnancies, ultrasound prenatal screening at 11–13 weeks plus 6 days also appears as an advantage compared to biochemistry testing, or maternal serum markers assessment at second trimester pregnancies. Therefore, current practices in clinical field are using ultrasonic prenatal examination, combining with maternal serum markers to assess the preliminary Trisomy 21 risk (Wee et al. 2010a; Nicolaides et al. 2008).

This book utilized the existing ultrasound imaging modality to improve the NT marker assessment in a semi-automated way while reducing human intervention. 3D volumetric images of NT are reconstructed for 3D boundary measurement rather than 2D weak echogenic lines.

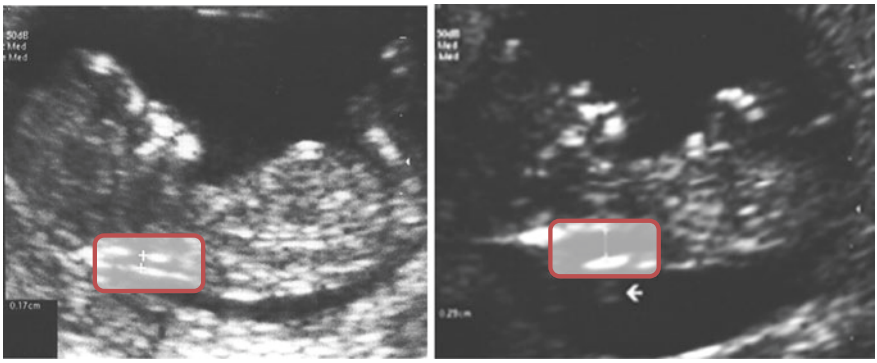

Fig. 2.8 Comparison of NT measurements with normal and high risk abnormal fetal: **b** Normal fetal 1.7 mm. **b** High risk abnormal fetal 2.9 mm

2.6 Two Dimensional Nuchal Translucency

In early 1990s, prenatal screening for high risk chromosomal defects such as Down's syndrome, triploidy, and Turner syndrome by using the combination of maternal age and NT thickness in the fetus within 11–13.6 weeks of gestation was introduced (Nicolaides et al. 1992, 1994). The term nuchal translucency (NT) was coined by Nicolaides et al. to describe the collection of fluid that is normally present behind the neck of the first trimester fetus. The stagnant fluids are obviously seen during 10–14 weeks gestation age, and then it will gradually decrease after 20 weeks and while making it difficult to detect the presence of key fold thickness. Fold thickness is a vital key marker to assess trisomy 21 of early pregnancy. 5 or 3.5 MHz abdominal ultrasound probe was used to scan the abdomen of pregnant women, where distance between fetal neck and the membrane cervical spine soft tissue in sagittal plane were measured as NT thickness. It should be essentially careful not to confuse the amniotic membrane as the layer of NT. According to FMF, NT measures considered abnormal were 3 mm and above and with 64 % sensitivity for trisomy 21 (Nicolaides et al. 1992). Figure 2.8 shows the example of normal and high risk abnormal ultrasonic NT thickness measurement.

2.6.1 Medicine Review and Related Researches

Meanwhile, some medical researchers claimed that fetus with large NT thickness (>3 mm) is associated with an increased risk for aneuploidy, congenital heart defect and other fetal anomalies (Hyett et al. 1995; Zosmer et al. 1999; Souka et al. 2001). Some publications also indicate that an increased NT thickness that is more than 2.5 mm in between 10 and 13 weeks plus 6 days has also been associated with an increased risk of congenital heart and genetic syndrome (Pandya

et al. 1994). Based on the past research in Harris Birthright research center for fetal medicine (Snijders et al. 1998), have coordinated the largest research to assess NT accuracy. It was conducted at 22 ultrasound centers in England on 96,127 women who were 10–14 weeks pregnant. The risk for trisomy 21 was calculated by multiplying the NT probability ratio by the prevalence of this trisomy at different maternal and gestational ages. Findings shows that 326 cases are found to be Trisomy 21 and among them, 231 cases or 71.2 % are found NT thickness are higher than 95th percentile. This has been proved that NT is the powerful marker for trisomy 21 screening. In 2004, the populations examined shows the definition of the minimum abnormal NT thickness is ranged from 2 to 10 mm (Nicholaides et al.). Prospective studies in more than 2,00,000 pregnancies which includes more than 900 Trisomy fetuses, indicates that NT screening assist in Trisomy detection for more than 75, with false positive rate of 5 % (FMF report). The importance of measuring NT as a screening tool can be evaluated from the fact that all over Europe, America and UK, NT measurement is included in their prenatal screening programs.

Hereafter the measurements of NT appear as a powerful screening marker during first trimester of pregnancy—early detection of abnormal findings in pregnancy is pivotal in establishing premature evaluation of chromosomes and possible structural defects on a targeted basis (Lee and Kim 2006). Trans-abdominal sonographic examinations are widely used to show the mid-sagittal image of the fetal neck to measure the nuchal fold. Trans-vaginal ultrasound of NT appears to be a more accurate method (Braithwaite and Economides 1995) due to increased resolution. Conversely, when using a trans-abdominal probe, the examiner possesses a wider range of maneuverability to obtain the correct mid-sagittal view of the fetus (Cullen et al. 1989). Fetal NT can be measured successfully by trans-abdominal ultrasound examination in about 95 % of cases; the rest cases are necessary to perform trans-vaginal sonography (FMF report). With the fact that NT thickness is known to be reliable marker for Trisomy 21 assessment, the ability to achieve a convinced measurement using manual B-mode ultrasound caliper is dependent on appropriate training and adherence to a standard technique in order to achieve uniformity of results among different operators.

Hence, fetal Medicine Foundation has promoted standardization in the assessment of NT which should follow the following criteria (FMF report); (a) Gestation should be between 11 and 13 +6 weeks, (b) Image is magnified so that head and upper thorax are included in the screen, (c) A mid sagittal view of fetal profile is obtained with ultrasound transducer being held parallel to longitudinal axis of nuchal translucency, (d) Crown hip length to be within the 45–84 mm, (e) Fetus must be in neutral position, as hyperextended or flexed neck will results 0.6 and 0.4 mm deviation respectively. (f) More than one measurement must be taken and maximum thickness in true sagittal plane is considered as NT thickness, (g) The calipers should place on lines that define NT thickness precisely; crossbar of caliper should be such that is hardly visible as it merges with the white line of the boundaries and not in the nuchal fluid. This is the most difficult requirement to realize under control. Generally, the

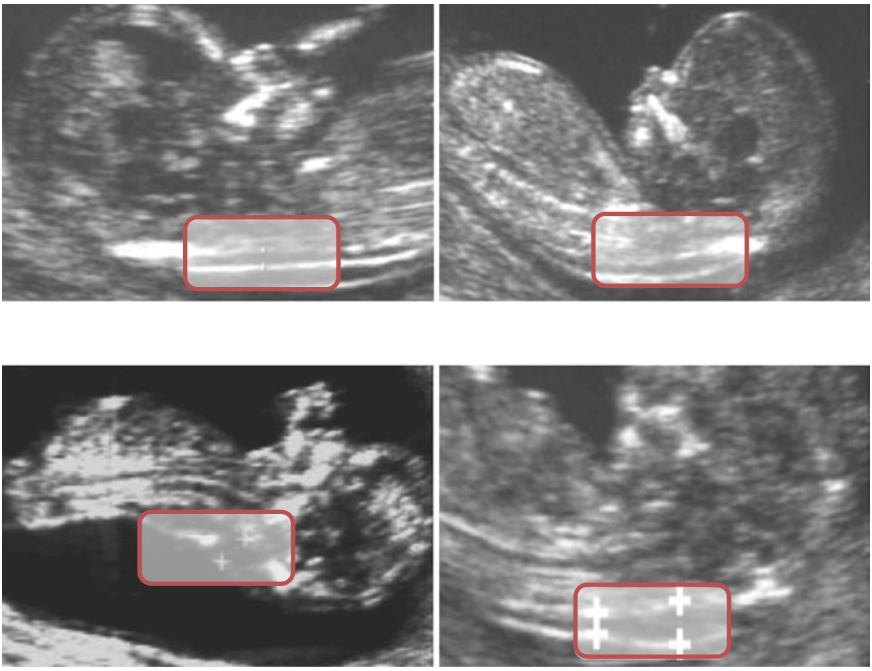

Fig. 2.9 Ultrasonic marker measurements; nuchal translucency at 12 weeks fetuses. **a** Correct measurement adhere to FMF protocol. **b** Hyperextended neck. **c** Flexed neck. **d** Maximum measurement of NT should be taken

measurement of fetal NT layer takes at least 15 min (Taipale et al. 1997), if the fetus is not in the right position, the overall prenatal screening will consume longer time. Figure 2.9 shows some example of NT measurement in different position and condition.

However, review of images by an experienced operator indicated that assessment may have been hampered either by poor magnification and unfavorable section or by untrained operator. As with screening based on NT, currently it is imperative that sonographers who undertake risk assessment by examination of fetal profile receive appropriate training and certification of their competence in performing such a scan. Reproducibility studies suggest that reproducibility of measurement is variable among groups and poor in some studies (Kanellopoulos et al. 2003; Bekker et al. 2004; Malone et al. 2004). It is possible that learning curve for this measurement is much longer for NT measurement (Cicero et al. 2003).

In some observational studies (Roberts et al. 1995; Kornman et al. 1996), the scans were often carried out at inappropriate protocol and the sonographers were either not trained adequately or they were not sufficiently motivated to measure NT. These methodological problems are further highlighted by a research of

Table 2.3 Correlation between nuchal translucency thickness, chromosomal abnormalities and alive well percentage

Nuchal translucency (mm)	Chromosomal abnormalities (%)	Alive well (%)
<95th centile	0.2	97
95–99th centiles	3.7	93
3.5–4.4	21.1	70
4.5–5.4	33.3	50
5.5–6.4	50.5	30
≥6.5	64.5	15

47,053 singleton pregnancies examined at 6–16 weeks (Wald et al. 2003). In 23 % of the patients no valid NT measurement was taken because the scans were carried out at inappropriate gestations or the sonographers were unable to obtain a measurement or none of the images were deemed to be of an acceptable quality.

2.6.1.1 Existing Limitation

From the medical researches earlier mention, it is known that trisomy 21 characteristic can be extracted from fetal ultrasound image with measured nuchal translucency thickness. Previous researches have concluded that minor inaccuracies in NT measurement as small as 25 % or 0.5 mm will have very significant negative impacts upon abnormality detection, reducing detection rates by 18 % (Moratalla et al. 2010; Abele et al. 2010). Table 2.3 summarized the correlation of nuchal translucency thickness with chromosomal abnormalities and alive well percentages.

Although FMF have developed a standardize protocol for NT assessment in 11 until 13 weeks + 6 days, it is recognized hardly to implement and practices in clinical implementation and realization. Inter and intra observer variability using conventional B-mode ultrasonic marker measurement (Pandya et al. 1995; Kanellopoulos et al. 2003) is still unavoidable. Accurate calipers placement on 2D echogenic lines boundaries are certainly a challenging problem, as shown in Fig. 2.10, therefore, the consistency of measurement cannot be guaranteed and always subject to human errors, technical difficulties, patient loads, and longer time consumptions.

2.6.2 Engineering Review and Related Researches

The application of ultrasound imaging to detect fetal abnormalities in early pregnancy has aroused great attention of genetic workers. There are also some related researches done in engineering field. Much attention now is focused on techniques to segment and measure NT marker only in 2D ultrasonic images. Efforts

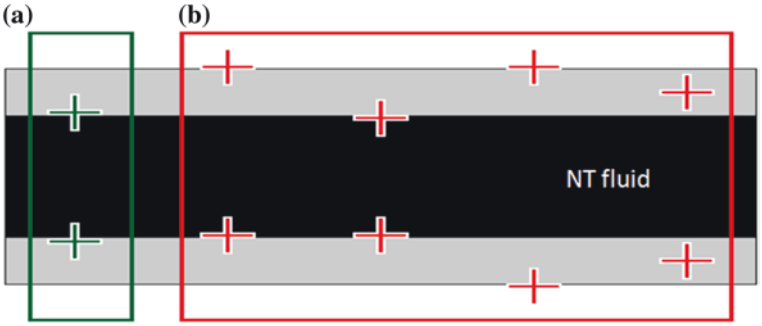

Fig. 2.10 Displacement of ultrasonic calipers for NT thickness boundary measurement. **a** Correct calipers placement. **b** Incorrect calipers placement

have been made by several investigators worldwide to try to find an approach for automation NT in two key procedures; first is the automatic distal and proximal echogenic lines detection and second is to measure the NT marker thickness in automated way, in order to reduce amount of human intervention. None of the 3D approaches dedicated for NT marker were found. In fact, there are very few papers dedicated on ultrasound imaging reporting automatic or semi-automatic NT measurement up to now. It reveals the fact that ultrasound fetal images are the difficult data to deal with, and therefore, the problem is still far from being solved until now.

The first scientific paper working on NT automation is Bernardino et al. 1998. They proposed simple image processing technique; histogram equalization for contrast enhancement and Sobel edge operator; to extract the upper and bottom echogenic lines of NT marker. The Sobel operator implements two 3 × 3 kernels which are convolved with the sources image; *A(i,j)* to calculate approximations of the derivatives—one for horizontal changes $h_x(i,j)$, and another for vertical $h_y(i,j)$ as shown below;

$$G(i,j) = \sqrt{\left(h_x^2(i,j) + h_y^2(i,j)\right)} \tag{2.5}$$

$$\theta(i,j)\ \text{arctanget}\left(\frac{h_x^2(i,j)}{h_y^2(i,j)}\right) \tag{2.6}$$

$$h_x = \begin{bmatrix} -1 & 0 & 1 \\ -2 & 0 & 2 \\ -1 & 0 & 1 \end{bmatrix} \;;\; h_y = \begin{bmatrix} 1 & 2 & 1 \\ 0 & 0 & 0 \\ -1 & -2 & -1 \end{bmatrix} \tag{2.7}$$

where, *G(i, j)* is the gradient magnitude, θ*(i, j)* is the gradient phase

This simple Sobel operator using a threshold specified by the user on the magnitude of the gradient for detection a variable number of image edges. But problem arise with no single image features can provide reliable NT boundaries for thickness measurement. The location of the edge is entirely determined by local

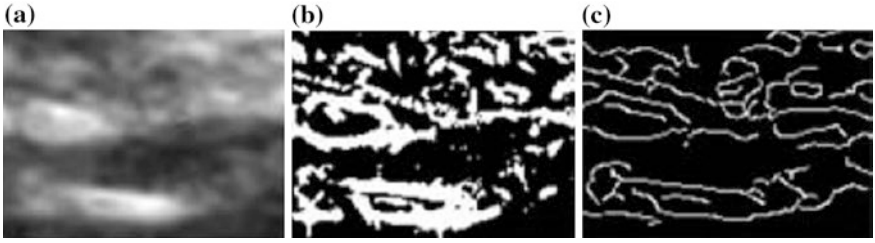

Fig. 2.11 Resultant of edge detection. **a** Original NT region of interest. **b** Sobel operator. **c** Canny operator

evaluation of single image feature such as the intensity or the intensity gradient. It is therefore impossible to detect the border of NT layer correctly in single image feature. Figure 2.11 illustrates the difficulty of simple edge operator implementing on ultrasonic images.

Conventional edge detection such as Sobel and Canny techniques has a drawback in NT measurement, as more than two echogenic lines will be mapped within the output image. A decade later, a method for semi-automated NT border measurements based on dynamic programming was proposed by Lee et al. in (2007). They presented a computerized method of detecting the border of NT layer by minimizing a cost function using dynamic programming. Thanks to the matured development of ultrasound speckle noise filter; nonlinear anisotropic diffusion techniques are implemented as their pre-processing before NT edge segmentation. The anisotropic diffusion filter having good characteristics to preserve NT image edge features while blurring the area inside the NT layer. The general diffusion equation proposed by Perona and Malik (1990) is as follows;

$$\frac{\partial I}{\partial t} = div\left(c\left(x, y, t\right)\nabla I\right) = \nabla c \cdot \nabla I + c\left(x, y, t\right)\Delta I \tag{2.8}$$

with the condition,

$$I\left(t = 0\right) \equiv I_0$$

where ∇ is the gradient operator, *div* is the divergence operator, *c(x, y)* is the diffusion coefficient, t is the diffusion time, $\Delta$is the Laplacian of I, and I_0 is the initial image. *C (t)* controls the rate of diffusion and is usually chosen as a function of the image gradient so as to preserve edges in the image. Perona and Malik proposed C (model) has the following two forms:

$$c(|\nabla I|) = \exp\left[-\left(\frac{|\nabla I|}{k}\right)^2\right] \tag{2.9}$$

$$c(|\nabla I|) = \frac{1}{1 + \left(\frac{|\nabla I|}{k}\right)^2} \tag{2.10}$$

where k is the edge magnitude factor, correlated to the contradiction degree's balance of edge preservation and smoothing factor, and final smoothing outcomes are influenced by diffusion time t. The basic idea of P-M model is using $c(|\nabla I|)$ to control the diffuse proliferation on the initial image. The model achieving adaptive diffusion based on image gradient magnitude. At the edges with large gradient modulus, $c(|\nabla I|)$whichever is less; the model is weak in smooth implementation to protect the edge information. In the homogenous areas gradient modulus is smaller, $c(|\nabla I|)$become larger; the model has more smoothing effect. Adaptive selection of smoothing degree at the edge and homogeneous region can help to identify the boundary location, and solved the contradiction between de-noising and edge retention.

For the NT layer segmentation, cost functions are built for each of the borders of the NT layer. Let's assumed all the possible borders B_n can be considered as polylines with n nodes;

$$B_n = \{P_1, P_2, P_3 \ldots, \ldots P_n\} \tag{2.11}$$

where $P_1, P_2, P_3 \ldots$ are the neighbouring pixels in x axis; n is the number of contours lines in horizontal length. Figure 2.12 illustrates the zone discrimination for NT image features and line border definition of B_1 and B_2.

The minimized cost function can be expressed as a sum of local costs along a candidate border B_N;

$$C(B_N) = C_f(P_1) = \sum_{i=2}^{N} (c_f(P_i) + C_g(P_{i-1}, P_i)) \tag{2.12}$$

When point $P_{i>1}$, local cost function terms $C_f(P_i)$ and $C_g(P_{i-1},P_i)$ are defined as follows;

$$C_f(P_i) = \sum_{j=1}^{k} w_j f_j(P_i) \qquad i = 1, \ldots, N \tag{2.13}$$

$$C_g(P_{i-1}, P_i) = W_{k+1} g(P_{i-1}, P_i) \tag{2.14}$$

$$g(P_{i-1}, P_i) = \left| d(P_i) - d(P_{i-1}) \right|^2 \quad i = 2, \ldots, N \tag{2.15}$$

By combining Eqs. 2.13, 2.14 and 2.15, minimized cost function is;

$$C(B_N) = C_f(P_1) + \sum_{i=2}^{N} \left(\sum_{j=1}^{k} w_j f_j(P_i) + w_{k+1} \left| d(P_i) - d(P_{i-1}) \right|^2 \right) \tag{2.16}$$

Where $f_j(P_i)$ are image feature terms, w_j is a weighting factor, $k = 3$ equal to the number of image features been considered, $|d(P_i) - d(P_{i-1})|^2$ is geometrical force term and d is the vertical distance between the border being estimated and a

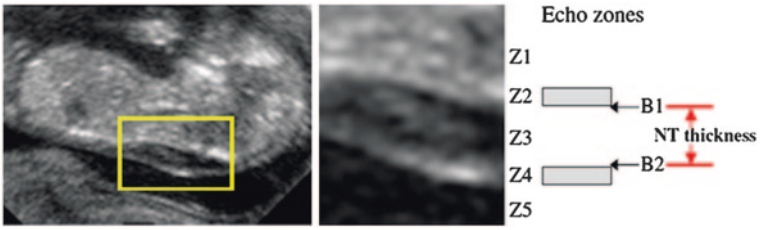

Fig. 2.12 NT border definitions and echo zones (Lee et al. 2007)

reference node. Their weighting factors are determined empirically for each border with relative constraint as follows;

$$|w_1| + |w_2| + |w_3| + |w_4| = 1 \tag{2.17}$$

According to the NT image features characteristics, referring to Fig. 2.12, the border B1 is below the bright region and above the dark region, meanwhile, border B2 is above the bright region and below the dark region. In other words, the characteristics of upper border B1 is opposite the lower border B2, therefore, weighting factors of image feature terms have to be opposite signs respectively. By considering this image feature characteristics, cost function $C(B_N)$ for B2 will be calculated in advanced by taking the horizontal line as reference line for $g(P_{i-1},P_i)$.

Based on Eq. 2.16, the first local cost term $f_1(P_i)$ measures the mean intensity of 3 pixels below a pixel P_i in order to detect a pixel above echo zone Z4. Second term $f_2(P_i)$ calculated the mean intensity of two pixels above a pixel P_i in order to detect a pixel below dark NT region at zone Z3. The third cost term $f_3(P_i)$ computed the downward intensity gradient at upper edge of echo zone Z4 by using vertical gradient operator $[1 \quad 0 \quad -1]^T$. For the final cost function term $g(P_{i-1},P_i)$ or $|d(P_i) - d(P_{i-1})|^2$, it is the vertical distance between the estimated border and a reference line for border continuity concern. For their proposed technique, B2 is calculated before B1; therefore, the estimating cost term $g(P_{i-1},P_i)$ in B1 control will take B2 as its reference line (Fig. 2.13).

The reason for Lee et al. (2007) to implement the DP back-tracking technique is to avoid local minima which could cause missed tracking of the optimum minimized cost function calculated previously. DP is commonly applied to optimize problems, in our case: tracing minimum cost term globally within the ROI in backward propagation horizontal polylines.

Although Lee's method improves the NT border continuity by local cost term $g(P_{i-1},P_i)$ and reduces the problem of operator variability using manual NT tracking and measurement, however, it remains several existing limitations; firstly, it does not solve the difficulty of true mid-sagittal plane selection which coincides with NT marker with maximum thickness: the plane selection work scope is pre-stage of their research data experimental simulation. Therefore, results of their semi-automated may underestimate the NT thickness; Second limitation is the choice of orientation for foetus position; their proposed technique can only

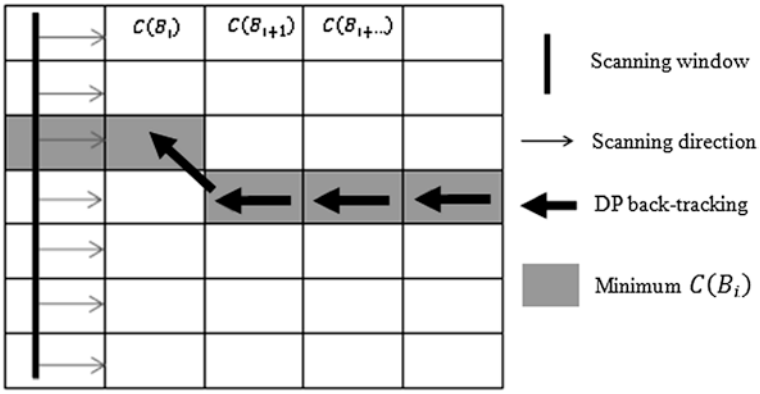

Fig. 2.13 Border line B2 detection using cost function $C(B_N)$ computation followed by dynamic programming (DP) back-tracking

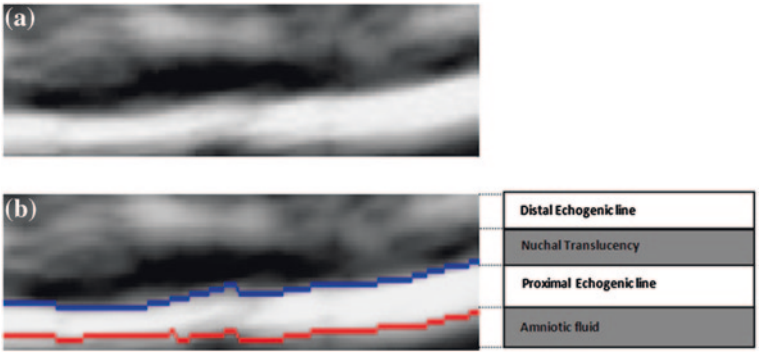

Fig. 2.14 Limitation of incorrect initiation line tracking. **a** Original NT ROI. **b** Missed tracked NT at proximal echogenic line

be applied on horizontal foetus position, which limits the method feasibility: the cost function $C(B_i)$ considers only horizontal neighbouring B_i node, therefore, DP back-tracking for global minimizes cost function in vertical NT position is not realizable.

Next, the manual cropping of NT region of interest (ROI) influences the automatic echogenic lines tracing heavily, their method is limit with fine ROI cropping excluding placenta beneath bottom NT line wisely, which is not the easy case in most of the ultrasonic images. Enlarged manual ROI cropping will change their weight factor characteristics as it refers to Fig. 2.12, simultaneously, final computation values of cost function for each pixel P_i can be changed. Hence, their NT layer are tracked one after another, by taking the first tracked line as reference line, if the initial first line was tracked at wrong position: bottom of proximal lines, consequently, second NT line will be tracked perfectly in wrong position. Figure 2.14 illustrates this limitation of incorrect initiated line and this leads to miss tracked NT layer.

Their proposed cost function calculation is heavily dependent on their weight factors, refer to Eq. 2.17, and the weights are not necessarily the same for both NT layers. Therefore, the choice of the cost function appears based on empiric consideration and it may further influent the quality of results explicitly.

Last but not least, the cost term $g(P_{i-1},P_i)$ for B2 distance calculation at pixel P_i from a reference line, which assumed as straight horizontal lines will cancel each other eventually. It only shows its effect when calculating cost term for B1, where previous tracked B2 will be taken as its reference line.

Due to this limitation, we have also proposed an iterative algorithm for both echogenic line borders simultaneous detection on 2D B-mode ultrasound images. The prior step of the proposed technique is the same with previous publication, which requires manual ROI containing NT layer thickness selection. Let's assume the acquired ROI is an $M \times N$ rectangle, and then all possible borders T_N are considered as polylines with N nodes:

$$T_n = \left[P_1, P_2, P_3, \ldots, P_{n-1}, P_n\right] \tag{2.18}$$

Where the pixels P_{n-1} and P_n are horizontal neighbors and n is the horizontal length of a contour line. The function of NT backbone $B(\Upsilon)$ is build according to reference point r, which is defined as follows:

$$\Upsilon_{1,2} = min\left[f(P_{1,n})\right] \tag{2.19}$$

The term $f(P_{1,n})$ measures the intensity gradient and intensity of pixels along P_1 and P_n, as shown in Fig. 2.15. Applied Eq. 2.19, the $B(\Upsilon)$ is formulated based on linear equation, as expressed follows:

$$\begin{aligned} y_j &= \nabla B(\Upsilon) x_i + \Upsilon_1 \\ i &= 1, \ldots n \quad j = \Upsilon_1, \ldots, \Upsilon_2 \end{aligned} \tag{2.20}$$

$$\nabla B(\Upsilon) = \frac{|\Upsilon_1 - \Upsilon_2|}{n} \tag{2.21}$$

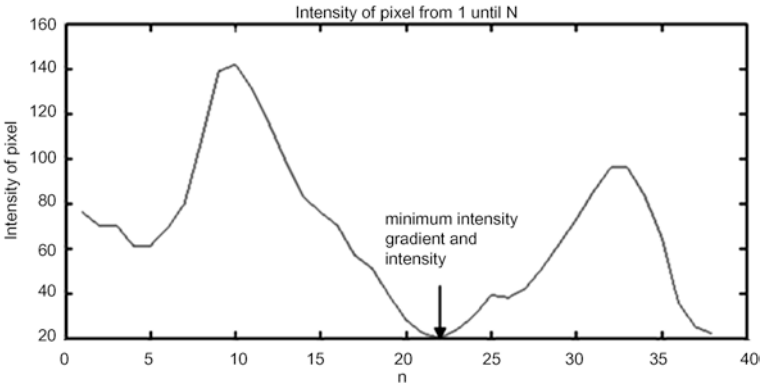

Fig. 2.15 Intensity gradients and intensity of pixels along P_1 and P_n

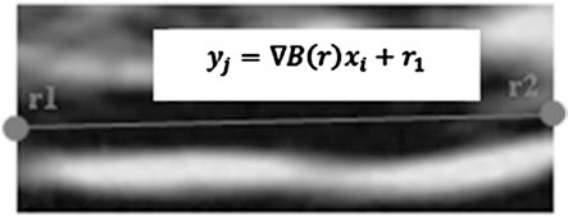

Fig. 2.16 Formation of NT backbone $B(\Upsilon)$ using both reference points Υ_1 and Υ_2

where x_i and y_j are the coordinate along this linear equation, Fig. 2.16 illustrates the linear equation coincide with both reference points Υ_1 and Υ_2.

The bidirectional forward propagation tracking process is used to scan through the NT edges of upper and lower boundaries within the $M \times N$ ROI referring to $B(\Upsilon)$, and stored in the array of T_{N1}, T_{N2}, as shown below;

$$T_{N1} = max\left[\nabla \text{ROI}\left(x_i, y_j - d_{1i}\right)\right] \tag{2.22}$$

$$T_{N2} = max\left[\nabla \text{ROI}\left(x_i, y_j - d_{2i}\right)\right] \tag{2.23}$$

where d_{1i} and d_{2i} are y-coordinates for maximum intensity gradient of both upper and lower border, the NT thickness was taken along every five pixels of polylines T_{N1} and T_{N2}. The maximum thickness of the subcutaneous translucency between skin and the soft tissue overlying the cervical spine should be measured. Therefore, the largest thickness is recorded as the NT measurement and calibrated with scale of ultrasound image to get the exact thickness in millimeter, as shown in Figs. 2.17, 2.18, 2.19.

Catanzariti et al. (2009) have also proposed an improved cost function for NT border segmentation. They modify the cost function in Eq. 2.12 by removing the weight factors, which indicative through empirical consideration. They believe this can help enhancing the automation process of NT layer measurement. Same to all previous semi-automated techniques, their proposed algorithm needs a manual NT ROI identification before introducing to their improved cost functions, as follows; Considering a NT ROI with dimensions $N \times M$, borders of polylines are;

$$B_N = \{P_1, P_2, P_3, \ldots, P_{N-1}, P_N,\} \tag{2.24}$$

where P_{N-1} and P_N are the adjacent pixels in horizontal; N equals to length of estimated border. Referring to Eq. 2.12, they have separated the cost function to two different functions for each upper and lower border respectively. The cost function to minimize lower border is as follows;

$$C_l(B_n) = C_l(B_{n-1}) + \left\{-\frac{\partial f}{\partial y}(P_n) + Z_l(P_n) + f_{\text{adj}}(P_n, P_{n-1})\right\} \tag{2.25}$$

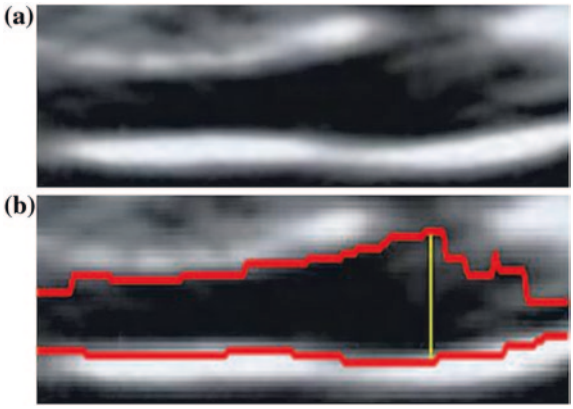

Fig. 2.17 Experimental result of maximum thickness NT measurement. **a** Sample original image. **b** Edge tracking and NT measurement

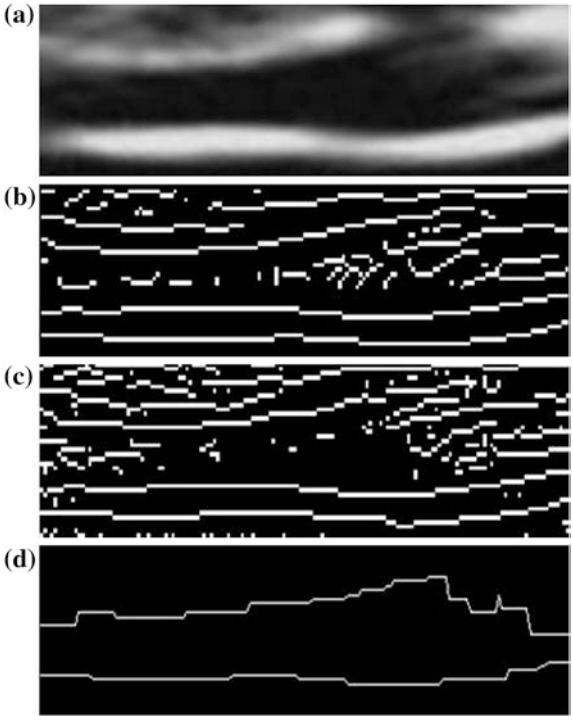

Fig. 2.18 Comparison of various edge detectors. **a** Original image. **b** Sobel detector. **c** Canny detector. **d** BIFP edge racing

where at node $n = 1$

$$C_l(B_1) = -\frac{\partial f}{\partial y}(P_1) + Z_l(x, y) \tag{2.26}$$

$$Z_l(p) = \begin{cases} 0 \; if \; \dfrac{\partial^2 f}{\partial \theta^2}(p) \times \dfrac{\partial^2 f}{\partial \theta^2}(t) < 0 \\ \varsigma \; otherwise \end{cases} \tag{2.27}$$

$$f_{adj}(P_n, P_{n-1}) = \begin{cases} 0 \text{ if } d(P_n, P_{n-1}) \leq 1 \\ \varsigma \ otherwise \end{cases} \tag{2.28}$$

The first local cost term $\frac{\partial f}{\partial y}(P_n)$ aims to replace both $f_1(P_i)$ and $f_2(P_i)$ at Eq. 2.13. It consists of the image derivative along vertical direction to consider the energy deriving from the image features as edges or lines. The second cost term is a second order derivatives computed along gradient direction, as a replacement for gradient operator $[1 \ 0 \ -1]^T$ proposed by Lee et al. (2007). Lastly, f_{adj} is built to replace $g(P_{i-1},P_i)$ term, to enforce borders continuity by penalising consecutive pixels distance larger than one pixel. Similar to Eq. 2.25, upper border cost function is built as follows;

$$C_u(B_n) = C_l(B_{n-1}) + \left\{ \frac{\partial f}{\partial y}(P_n) + Z_u(P_n) f_{\text{adj}}(P_n, P_{n-1}) + f_{\text{pos}}(B_n, B_n) \right\} \tag{2.29}$$

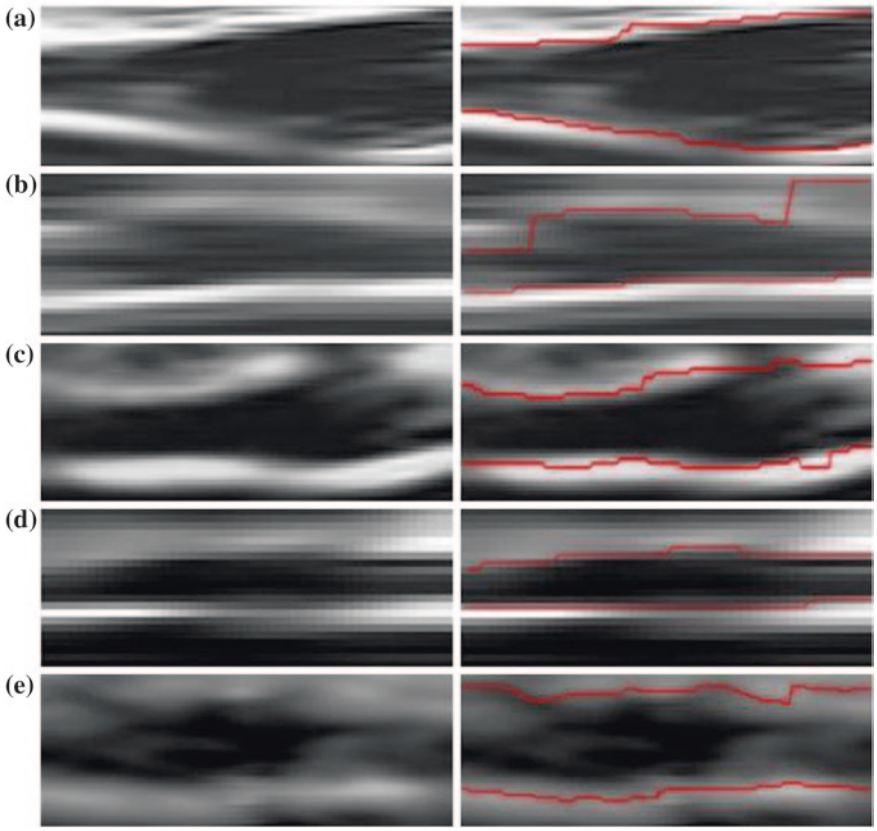

Fig. 2.19 Experimental results on 2D B-mode Ultrasonic NT images, left are original sample images, right are the findings of BIFP algorithm

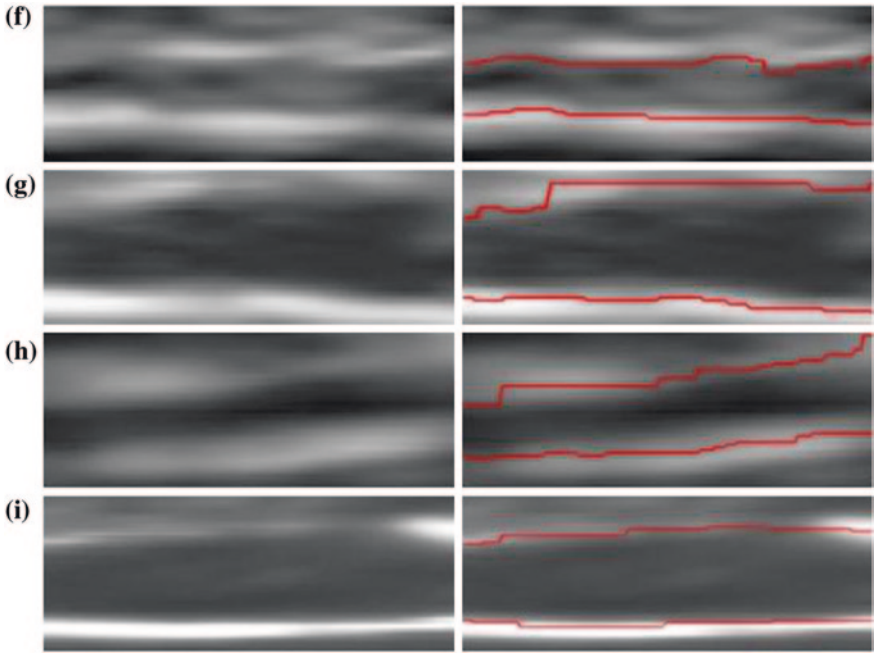

Fig. 2.19 Continued above

where at node $n = 1$

$$C_u(B_1) + \left\{ \frac{\partial f}{\partial y}(P_1) + Z_u(x, y) + f_{\text{pos}}(B_1, P_1) \right\} \tag{2.30}$$

$$Z_u(p) = \left\{ 0 \text{ if } \frac{\partial^2 f}{\partial \theta^2}(p) \times \frac{\partial^2 f}{\partial \theta^2}(q) < 0 \atop \varsigma \; otherwise \right\} \tag{2.31}$$

By observing both Eqs. 2.25 and 2.29, a new local term is introduced exclusively for upper border cost function. This term consists of a sigmoidal function which weighs the relative pixels distance between upper border and its corresponding lower border, therefore, it constrains the estimated upper border is stay above the lower NT border.

The advantage from their modified cost function is that, it is general; as it does not depend on weight tuning for each image. Nevertheless, it is still inherent with others existing limitation from Lee's method includes true sagittal plane selection; enlarged ROI manual cropping and fetus position.

Since late 2010, the first commercial tool of semi-automated 2D NT measurement system is called SonoNT^{TM} using GE Voluson 730 Expert (RAB 4-8L probe, Milwaukee, WI, USA) was reported. Moratalla et al. (2010) and Abele et al. (2010) have implemented this new commercial tool to investigate the operator inter and intra variability, and compared to conventional NT manual measurement method.

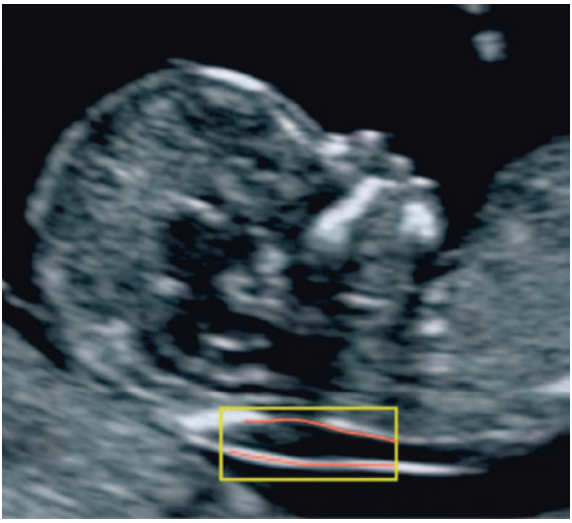

Fig. 2.20 Semi-automated process of SonoNT^{TM}, box placed by operator and the lines draw by system automatically (Moratalla et al. 2010)

An adjustable box has to be placed on relevant area at the back of the fetal neck, where the semi-automated system will interrogates the whole length of nuchal membrane within the marked box and draws the edge lines through the center of nuchal membrane and soft tissue overlying cervical spines respectively. This system utilizes the gradient and brightness information inside the box to define their drawing lines. Unfortunately, due to its commercial copyright and patents, details of their algorithms are not reported. Figure 2.20 illustrates the process of SonoNT^{TM} to measure NT thickness. In order to calculate the vertical distance of NT thickness, each point on one line is virtually connected to all possible points on the other line, the final NT length is the longest among all the minimum distances between the lines.

The vital key difference of this new commercial NT tool as compared to the previous gold standard developed by FMF; the automated drawing line that defines the edge of NT layer are laid on the centre of nuchal membrane rather than at its inner border. This is due to their system requirement to magnify the ultrasound fetal images (either pre- or post-freeze zoom) which results in thickening of the lines that defines fetal NT. Consequently, the translucent area between NT layers become smaller and may lead to measurement underestimation. This phenomenon was not reported in the studies since early 1990s. It is believed that pre-processing and post-processing imaging by latest GE US system which it includes speckle reduction imaging (SRI) and harmonics application contribute to the factor of thickening membrane lines (Moratalla et al. 2010). Therefore, the GE healthcare technology segments the NT border at the point of maximum echogenicity which normally lies in the centre of membrane lines. This is different with the measurement protocol developed by FMF Fig. 2.21.

Issue on relying SonoNT^{TM} to measure NT thickness and replace expertise have arisen an argument; blasphemy or oblation to quality, as reported by Ville (2010). It is exposed to two main types of drift from the expected clinical and

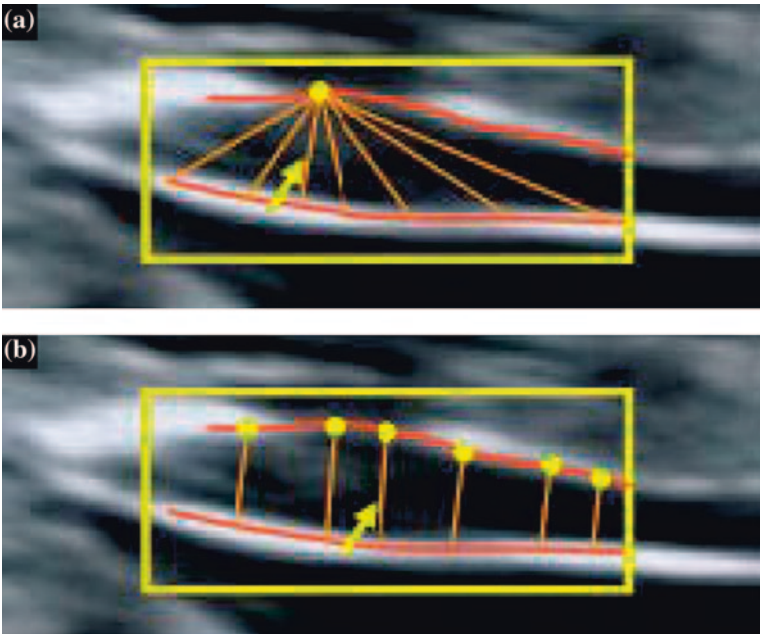

Fig. 2.21 Nuchal translucency thickness measurement. **a** Virtual points connection for minimum distance calculation. **b** Longest length among minimum distance lines is considered as NT thickness (Moratalla et al. 2010)

economics benefits; misuse and abuse of automation. Abuse occurs when the design function does not fit the clinical expectation, and misuse arises when operator overreliance on automation and their role becomes by-product of automation. Crude errors in NT measurements are generated by this semi-automated system if the selected ROI box encompasses more of nuchal area; this is the same typical error for all previous described semi-automated NT researches (Lee et al. 2007; Catanzariti et al. 2009; Bernardino et al. 1998). Figure 2.22 illustrates the example of semi-automated measurement error.

Furthermore, one argues that this semi-automation system is not useful for well-trained operators, as each individual interprets results differently. Yet, it is still questionable to accept this new method when there is no published references range, as compared to the FMF method which establishes through cumulative studies over the last 10 years.

2.6.2.1 Summary

Among all previous engineering work done, dedicated on automatic or semi-automatic fetal measurements, research topics are focused on nuchal translucency thickness segmentation and measurement using 2D ultrasonic images.

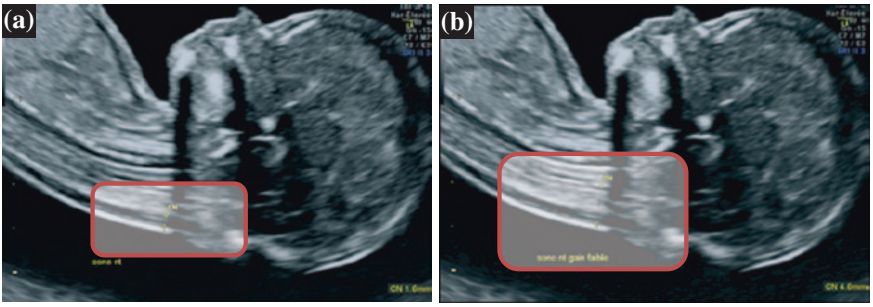

Fig. 2.22 False reading when larger ROI box placed over nuchal area. **a** Correct NT measurement 1.6 mm with fit ROI box. **b** Abuse NT measurement 4.6 mm with larger ROI box. (Ville 2010)

However, manipulation of true mid-sagittal plane selection was never resolved in which causing underestimation of NT thickness, while the position of fetus is limited to horizontal position and limitation of manual NT ROI cropping excluding non NT layer region.

These reveal that the existing methodological problems needs a 3D computing for NT measurement, in which measured 3D NT structure appears explicit assembly as compared to 2D inherent lines boundary. The current sonographer picks the three best 2D sagittal planes upon on their experiences using hand-eye coordination, and average of three NT measurements is taken as the final marker thickness. This inefficiency can be resolved within 3D NT reconstruction and incorrect plane selection can be avoided. Besides, with existing 2D images only the recorded images can be reviewed, even minor changes cannot be made. With 3D NT approaches, the actual viewing planes can be manipulated using the reconstructed saved volume data; the NT measurement can be re-calculated to aid reassessments and validation.

Our efforts are to find an approach for boundary detection in ultrasonic NT images which is less reliant on human operators. As it reduces the amount of human intervention, it will also reduce inter-observer variability and the intra-observer variability is expected to be reduced; consequently, drifting problem in measurements over time in longitudinal studies is reduced. Therefore, we have extended the current NT measurement from 2D ultrasonic marker to 3D volumetric ultrasound in order to overcome all the limitations above.

2.7 Three Dimensional Ultrasound Applications

With continuous improvement of ultrasound equipment and innovative technology in current research and development, three-dimensional (3D) ultrasound technology has been used in clinical research and diagnosis, particularly in prenatal care aspects. In late 1980's, 3D ultrasound imaging becomes reality due to the rapid development

of computing technology in terms of both hardware and software. There are three different 3D ultrasound imaging visualization, which includes surface rendering, transparent volumetric rendering and multi-planar reformatting (MPR). Nevertheless, the visualization of these 3D ultrasound imaging are still heavily influenced by quality of the 2D image. In the early 1990s, 3D images of first trimester pregnancies were presented (Bonilla-Musoles et al. 1995; Kelly et al. 1992).

3D medical images have been found to be more valuable and powerful fetal diagnostic tool (Fenster et al. 2001). The visualization of conventional 2D medical data is rather trivial while visualization of 3D volumetric data is not (Wee et al. 2011). The major application of 3D ultrasound in current prenatal screening tends to inspect qualitative physical abnormalities and quantitative masked volume measurement. Qualitatively, much of these work have been concerned with the detection of fetal physical abnormalities (Baba et al. 1999), for instance: facial, cleft lips, limb and other physical anatomy development (Lee et al. 1995). In 1995, Nelson and Pretorius have been using 3D ultrasound imaging to evaluate skeletal dysplasia, abnormalities leading to a small thorax and neural tube defects (NTD). NTD is a failure developing fetal spine which do not close properly, resulting anencephaly and spina bifida.

Quantitatively, the 3D measurements are mostly focused on masked volume estimation of placental, fetal and gestational sac (Blaas et al. 1998; Hafner et al. 1998). The estimated ROI volumes are either masked manually for multiple, individual slices or by masking a structure that has been isolated using an editing tool. Previous researches have reported 3D ultrasound imaging for volume measurement of fetal lumbar spine (Schild et al. 1999), fetal volume and weight estimation (Rankin et al. 1993), fetal liver (Laudy et al. 1998), and fetal lung (Pohls and Rempen 1998). Another concern of obstetrics volume measurement is placental volume around mid-pregnancy for birth weight estimation (Howe et al. 1994). Besides, the usages of trans-vaginal 3D ultrasound have been reported to investigate embryos shape and volume during early pregnancy (Blaas et al. 1998). However, in Malaysia, 3D ultrasound scanning is not covered in the routine prenatal screening protocol.

In addition to obstetrics and gynecology application, the usefulness of 3D ultrasound imaging has also reported to cover range from neurology (Rankin et al. 1993) for tumors diagnostics during brain surgery; neonatal ventricular volume measurement (Nagdyman et al. 1999; Kampmann et al. 1998) to cardiology (Martin et al. 1990; Arbeille et al. 2000; Gopal et al. 1997; Ofili and Nanda 1994; Salustri and Roelandt 1995; Magni et al. 1996). Some reports show high feasibility in 3D volume visualization and measurement for accurate atherosclerotic plaques diagnostics (Fenster and Downey et al. 1996; Rosenfield et al. 1992; Allott et al. 1999), prostate gland volume measurement (Aarnink et al. 1995; Basset et al. 1991; Nathan et al. 1996; Terris and Stamey 1991), breast imaging (Fenster and Downey 1996; Fenster et al. 1995), and ophthalmology (Downey et al. 1996).

Among all the previous literatures, 3D ultrasound techniques are not widely applied on NT application. Clinical personnel follow the gold standard developed by FMF for B-mode ultrasonic NT marker measurement despite it contains

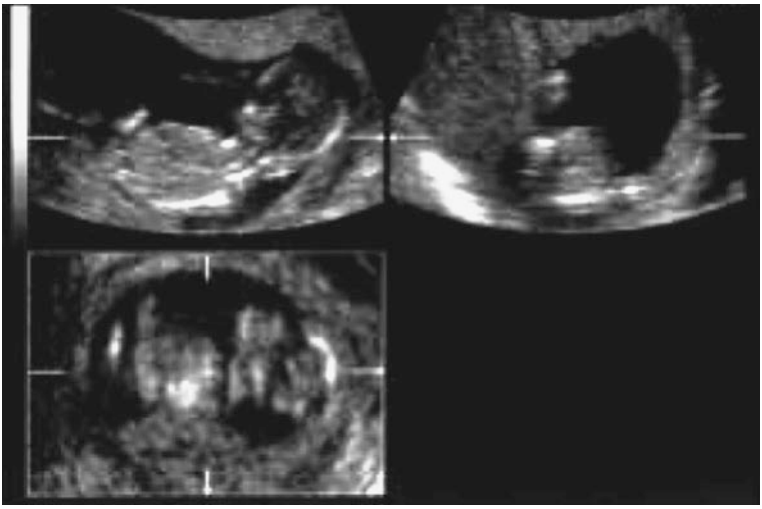

Fig. 2.23 NT measurements (2D) using Multi-planar reformatting (MPR) (Paul et al. 2001)

the described limitation in previous summaries section. In 2001 Paul et al. claims to measure NT thickness using 3D ultrasound imaging; however, their studies show that their measurement were conducted on re-slicing 2D ultrasound image from 3D multi-planar (MPR) visualization; sagittal, coronal and axial view plane. 2D measurements were taken rather than 3D thickness measurement, which in fact it makes no difference from conventional B-mode NT assessment. However, position of mid-sagittal plane selection can be known. Figure 2.23 illustrates their MPR measurement on 2D re-slice fetal images, rather than using 3D volume rendering measurement. Figure 2.24 illustrates the example of our 3D volume rendering measurement.

Furthermore, fully 3D acquisition systems are not widespread due to technological and economic reasons, especially in developing countries, and the majority of US scanners are freehand systems acquiring 2D B-scan images. Therefore, a software methodology for obtaining a 3D NT reconstruction and interactive visualization based on these systems is highly desirable.

2.7.1 Summary

With the rapid build-up of medical informatics technology and development, the demand on various sophisticated medical equipment are increasing dramatically. Nevertheless, many developing countries such as Malaysia are heavily depending on imported medical equipment, needless to say, the high cost reduces the treatment opportunity for the majority patients. This difficulty remains unsolved and limits patient category with only high income earners

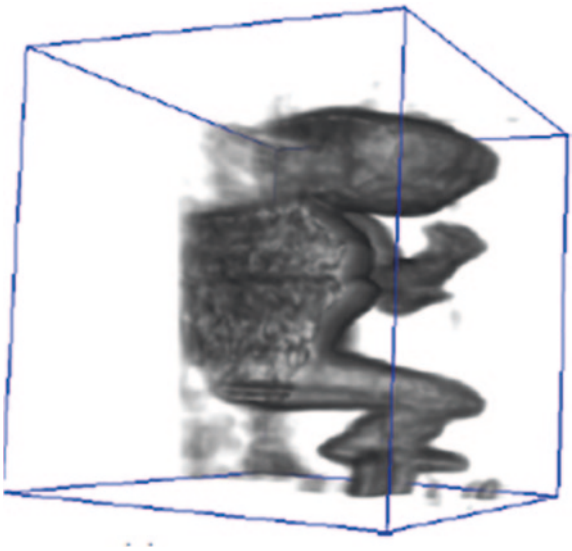

Fig. 2.24 Example of our simulated 3D volumetric rendering ultrasound fetal images

having easy access to benefits from high end medical technologies. This book proposed the techniques integrated with conventional 2D ultrasound systems in order to yield 3D interactive system dedicated for NT visualization system with no extra cost.

Generally, the ultrasound machines prices start at about RM 30,000 for 2D system and may range up to RM 700,000 for 3D or 4D system. A small heath center can purchase a simple B mode ultrasound machine on the very low end of this price range while a large hospital might pay nearly a million ringgit for a color machine with 4D images capability. The price difference between systems could rise up to 90 % high which depends largely on the level of technology. On the other hand, currently, many large-scaled hospitals, DICOM images are embedded in 3D reconstruction software which is similar to a class of large-scale image processing workstation or treatment planning system. A major drawback of the workstation system is the great consumption of computing processing. Therefore, to perform the task, demanding hardware configuration is needed and thus led to a rise of cost. Consequently, the establishment of such workstation is not affordable for most of the small-scaled hospitals. By virtue of its ineffectiveness, developer companies hardly to be benefited from the routine maintenance.

Besides, it is clear that 3D ultrasound has not been yet gained widespread of clinical acceptance. Most of the literatures presented reveal an emphasis on research projects, which extremely rarely and limitedly covered in routine protocol. It is used as a specialist laboratory tools for specific syndrome investigation, this is because the effort required to obtain high quality 3D ultrasound data often outweighs the potential benefits.

Another difficulty of 3D US fetal imaging is due to the fetus movement during scanning process. The automatic 3D probe mechanical movement may cover the images of fetus movement, especially in longer scanning time. This is the reason why 3D US system are not quantitatively reported for fetal biometrics measurement using existing commercial 3D probes except volume masking and its estimation. When medical personnel are not satisfied with the 3D scanning results, rescan is often performed. Hence, common 3D ultrasound probe operated at high frequencies for higher resolution will lower the penetration ability of the sound waves, i.e. 12 for 4D mode, 8 MHz for 3D mode. Apparently, proximal and distal NT layer beneath fetus neck is hardly assessable using high frequencies ultrasound setting. This limitation will be encountered in our research where conventional 3.5 MHz trans-abdominal probe is applied.

In present research, we have proposed a 3D ultrasound reconstruction and visualization for a specific ultrasound marker, namely nuchal translucency or NT, which is the important measurement parameter to assess the risk of trisomy 21 in early pregnancy. Measurements of NT were conducted in 3D spaces through the proposed state-of-art computerized algorithms. The proposed method has encountered the difficulty of current manual assessment method on using conventional B mode ultrasonic images. New visualization techniques have made it possible to create 2D cross sections that were not obtainable at regular scanning by processing a block of volume data (arbitrary slicing), presenting the surface of an object (surface shading), and looking into an object (transparency mode). Hence, it should be understood that due to the characteristics of NT marker anatomy, 3D thickness measurement on 3D structure with existing commercial ultrasound machine is not available. This project aims to design a non-invasive Trisomy 21 screening method easier for operator, at the same time, more robust removing the issues arise by FMF gold standard protocol. 3D visualization and measurement of ultrasound marker NT will be developed with the aim to improve the findings accuracy and consistency.

References

Aarnink, R. G., Huynen, A. L., Giesen, R. J. B., Delarosette, J., Debruyne, F. M. J., & Wijkstra, H. (1995). Automated prostate volume determination with ultrasonographic imaging. *Journal of Urology, 153*(5), 1549–1554.

Abele, H., Hoopmann, M., Wright, D., Hoffmann-Poell, B., Huettelmaier, M., Pintoffl, K., et al. (2010). Intra- and interoperator reliability of manual and semi-automated measurement of fetal nuchal translucency by sonographers with different levels of experience. *Ultrasound in Obstetrics and Gynecology, 36*(4), 417–422.

Abuhamad, A. (2005). Technical aspects of nuchal translucency measurement. *Seminars in Perinatology, 29*(6), 376–379.

Allott, C. P., Barry, C. D., Pickford, R., & Waterton, J. C. (1999). Volumetric assessment of carotid artery bifurcation using freehand-acquired, compound 3D ultrasound. *British Journal of Radiology, 72*(855), 289–292.

Arbeille, P., Eder, V., Casset, D., Quillet, L., Hudelo, C., & Herault, S. (2000). Real-time 3-D ultrasound acquisition and display for cardiac volume and ejection fraction evaluation. *Ultrasound in Medicine and Biology, 26*(2), 201–208.

Baba, K., Okai, T., Kozuma, S., & Taketani, Y. (1999). Fetal abnormalities: evaluation with real-time-processible three-dimensional US—preliminary report. *Radiology, 211*(2), 441–446.

Basset, O., Gimenez, G., Mestas, J. L., Cathignol, D., & Devonec, M. (1991). Volume measurement by ultrasonic transverse or sagittal cross-sectional scanning. *Ultrasound in Medicine and Biology, 17*(3), 291–296.

Bekker, M. N., Twisk, J. W. R., & van Vugt, J. M. G. (2004). Reproducibility of the fetal nasal bone length measurement. *Journal of Ultrasound in Medicine, 23*(12), 1613–1618.

Bernardino, F., Cardoso, R., Montenegro, N., Bernardes, J., & de Sa, J. M. (1998). Semiautomated ultrasonographic measurement of fetal nuchal translucency using a computer software tool. *Ultrasound in Medicine and Biology, 24*(1), 51–54.

Blaas, H. G., Eik-Nes, S. H., Berg, S., & Torp, H. (1998). In vivo three-dimensional ultrasound reconstructions of embryos and early fetuses. *Lancet, 352*(9135), 1182–1186.

Bonillamusoles, F., Raga, F., Osborne, N. G., & Blanes, J. (1995). Use Of 3-dimensional ultrasonography for the study of normal and pathological morphology of the human embryo and fetus—preliminary-report. *Journal of Ultrasound in Medicine, 14*(10), 757–765.

Braithwaite, J. M., & Economides, D. L. (1995). The measurement of nuchal translucency with transabdominal and transvaginal sonography—success rates, repeatability and levels of agreement. *British Journal of Radiology, 68*(811), 720–723.

Bulletins, A. C. o. P. (2007). Acog practice bulletin no. 77: Screening for fetal chromosomal abnormalities. *Obstetrics and gynecology, 109*(1), 217–227.

Catanzariti, E., Fusco, G., Isgrò, F., Masecchia, S., Prevete, R., & Santoro, M. (2009). A semi-automated method for the measurement of the fetal nuchal translucency in ultrasound images.

Cicero, S., Bindra, R., Rembouskos, G., Spencer, K., & Nicolaides, K. H. (2003a). Integrated ultrasound and biochemical screening for trisomy 21 using fetal nuchal translucency, absent fetal nasal bone, free Beta-Hcg and Papp-A At 11 To 14 weeks. *Prenatal Diag, 23*(4), 306–310.

Cicero, S., Dezerega, V., Andrade, E., Scheier, M., & Nicolaides, K. H. (2003b). Learning curve for sonographic examination of the fetal nasal bone at 11–14 weeks. *Ultrasound in Obstetrics and Gynecology, 22*(2), 135–137.

Cullen, M. T., Green, J. J., Reece, E. A., & Hobbins, J. C. (1989). A comparison of trans-vaginal and abdominal ultrasound in visualizing the 1st trimester conceptus. *Journal of Ultrasound in Medicine, 8*(10), 565–569.

Down, J. L. (1995). Observations on an Ethnic classification of idiots. *Mental Retardation, 33*(1), 54–56.

Downey, D. B., Nicolle, D. A., Levin, M. F., & Fenster, A. (1996). Three-dimensional ultrasound imaging of the eye. *Eye, 10*, 75–81.

Fenster, A., & Downey, D. B. (1996). 3-D ultrasound imaging: a review. *IEEE Engineering in Medicine and Biology Magazine, 15*(6), 41–51.

Fenster, A., Tong, S., Sherebrin, S., Downey, D. B., & Rankin, R. N. (1995). Three-dimensional ultrasound imaging. *Proceedings of SPIE, 2432*, 176–184.

Fenster, A., Downey, D. B., & Cardinal, H. N. (2001). Three-dimensional ultrasound imaging. *Physics in Medicine & Biology, 46*(5), R67–R99.

Gopal, A. S., Schnellbaecher, M. J., Shen, Z. Q., Akinboboye, O. O., Sapin, P. M., & King, D. L. (1997). Freehand three-dimensional echocardiography for measurement of left ventricular mass: in vivo anatomic validation using explanted human hearts. *Journal of the American College of Cardiology, 30*(3), 802–810.

Hafner, E., Philipp, T., Schuchter, K., Dillinger-Paller, B., Philipp, K., & Bauer, P. (1998). Second-trimester measurements of placental volume by three-dimensional ultrasound to predict small-for-gestational-age infants. *Ultrasound in Obstetrics and Gynecology, 12*(2), 97–102.

Howe, D., Wheeler, T., & Perring, S. (1994). Measurement of placental volume with real-time ultrasound in mid-pregnancy. *Journal of Clinical Ultrasound, 22*(2), 77–83.

Huether, C. A., Ivanovich, J., Goodwin, B. S., Krivchenia, E. L., Hertzberg, V. S., Edmonds, L. D., et al. (1998). Maternal age specific risk rate estimates for down syndrome among live births in whites and other races from Ohio and Metropolitan Atlanta, 1970–1989. *Journal of Medical Genetics, 35*(6), 482–490.

Hyett, J. A., Moscoso, G., & Nicolaides, K. H. (1995). Cardiac defects in 1st-trimester fetuses with trisomy 18. *Fetal Diagnosis and Therapy, 10*(6), 381–386.

Kagan, K. O., Wright, D., Spencer, K., Molina, F. S., & Nicolaides, K. H. (2008). First-trimester screening for trisomy 21 by free beta-human chorionic gonadotropin and pregnancy-associated plasma protein-A: Impact of maternal and pregnancy characteristics. *Ultrasound in Obstetrics and Gynecology, 31*(5), 493–502.

Kagan, K. O., Cicero S., et al (2009). Fetal nasal bone in screening for trisomies 21, 18 and 13 and Turner syndrome at 11–13 weeks of gestation. *Ultrasound in Obstetrics and Gynecology, 33*(3):259–264.

Kampmann, W., Walka, M. M., Vogel, M., & Obladen, M. (1998). 3-D sonographic volume measurement of the cerebral ventricular system: In vitro validation. *Ultrasound in Medicine and Biology, 24*(8), 1169–1174.

Kanellopoulos, V., Katsetos, C., & Economides, D. L. (2003). Examination of fetal nasal bone and repeatability of measurement in early pregnancy. *Ultrasound in Obstetrics and Gynecology, 22*(2), 131–134.

Kelly, I. M. G., Gardener, J. E., & Lees, W. R. (1992). 3-Dimensional Fetal Ultrasound. *Lancet, 339*(8800), 1062–1064.

Kornman, L. H., Morssink, L. P., Beekhuis, J. R., deWolf, B., Heringa, M. P., & Mantingh, A. (1996). Nuchal translucency cannot be used as a screening test for chromosomal abnormalities in the first trimester of pregnancy in a routine ultrasound practice. *Prenatal Diag, 16*(9), 797–805.

Laudy, J. A. M., Janssen, M. M. M., Struyk, P. C., Stijnen, T., Wallenburg, H. C. S., & Wladimiroff, J. W. (1998). Fetal liver volume measurement by three-dimensional ultrasonography: a preliminary study. *Ultrasound in Obstetrics and Gynecology, 12*(2), 93–96.

Lee, Y.-B., & Kim, M.-H. (2006). Automated ultrasonic measurement of fetal nuchal translucency using dynamic programming. In J. Martínez-Trinidad., J. A. Carrasco Ochoa., & J. Kittler. (Eds.), *Progress in Pattern Recognition, Image Analysis and Applications* (Vol. 4225, pp. 157–167), Berlin/Heidelberg: Springer.

Lee, A., Deutinger, J., & Bernaschek, G. (1995). 3-dimensional ultrasound—abnormalities of the fetal face in surface and volume rendering mode. *British Journal of Obstetrics and Gynaecology, 102*(4), 302–306.

Lee, Y.-B., Kim, M.-J., & Kim, M.-H. (2007). Robust border enhancement and detection for measurement of fetal nuchal translucency in ultrasound images. *Medical & Biological Engineering & Computing, 45*(11), 1143–1152.

Leshin, L. (1997). *Trisomy 21: The story of down syndrome*. Health Issues: D-S health Down Syndrome.

Magni, G., Cao, Q. L., Sugeng, L., Delabays, A., Marx, G., Ludomirski, A., et al. (1996). Volume-rendered, three-dimensional echocardiographic determination of the size, shape, and position of atrial septal defects: validation in an in vitro model. *American Heart Journal, 132*(2), 376–381.

Malone, F. D., Ball, R. H., Nyberg, D. A., Comstock, C. H., Saade, G., Berkowitz, R. L., Dugoff, L., Craigo, S. D., Carr, S. R., Wolfe, H. M., Tripp, T., D'Alton, M. E., & Consortium, F. R. (2004). First-trimester nasal bone evaluation for aneuploidy in the general population. Obstetrics and gynecology, *104*(6), 1222–1228.

Martin, R. W., Bashein, G., Detmer, P. R., & Moritz, W. E. (1990). Ventricular volume measurement from a multiplanar transesophageal ultrasonic-imaging system—an invitro study. *IEEE Transactions on Biomedical Engineering, 37*(5), 442–449.

Moratalla, J., Pintoffl, K., Minekawa, R., Lachmann, R., Wright, D., & Nicolaides, K. H. (2010). Semi-automated system for measurement of nuchal translucency thickness. *Ultrasound in Obstetrics and Gynecology, 36*(4), 412–416.

Nagdyman, N., Walka, M. M., Kampmann, W., Stöver, B., & Obladen, M. (1999). 3-D ultrasound quantification of neonatal cerebral ventricles in different head positions. *Ultrasound in Medicine and Biology, 25*(6), 895–900.

Nathan, M. S., Seenivasagam, K., Mei, Q., Wickham, J. E. A., & Miller, R. A. (1996). Transrectal ultrasonography: Why are estimates of prostate volume and dimension so inaccurate? *British Journal of Urology, 77*(3), 401–407.

Nicolaides, K. H., Azar, G., Byrne, D., Mansur, C., & Marks, K. (1992). Fetal nuchal translucency: ultrasound screening for chromosomal defects in first trimester of pregnancy. *BMJ, 304*(6831), 867–869.

Nicolaides, K. H., Brizot, M. L., & Snijders, R. J. M. (1994). Fetal nuchal translucency—ultrasound screening for fetal trisomy in the first trimester of pregnancy. *British Journal of Obstetrics and Gynaecology, 101*(9), 782–786.

Nicolaides, K., Sebire, N., & Snijders, R. (1999). *The 11–14 weeks scan: the diagnosis of fetal abnormalities*. New York, NY: Parthenon Publishing.

Nicolaides, K. H., Kagan, K. O., Wright, D., Baker, A., & Sahota, D. (2008). Screening for trisomy 21 by maternal age, fetal nuchal translucency thickness, free beta-human chorionic gonadotropin and pregnancy-associated plasma protein-A. *Ultrasound in Obstetrics and Gynecology, 31*(6), 618–624.

Ofili, E. O., & Nanda, N. C. (1994). 3-dimensional and 4-dimensional echocardiography. *Ultrasound in Medicine and Biology, 20*(8), 669–675.

Pandya, P. P., Brizot, M. L., Kuhn, P., Snijders, R. J. M., & Nicolaides, K. H. (1994). First-trimester fetal nuchal translucency thickness and risk for trisomies. *Obstetrics and Gynecology, 84*(3), 420–423.

Pandya, P. P., Altman, D. G., Brizot, M. L., Pettersen, H., & Nicolaides, K. H. (1995). Repeatability of measurement of fetal nuchal translucency thickness. *Ultrasound in Obstetrics and Gynecology, 5*(5), 334–337.

Paul, C., Krampl, E., Skentou, C., Jurkovic, D., & Nicolaides, K. H. (2001). Measurement of fetal nuchal translucency thickness by three-dimensional ultrasound. *Ultrasound in Obstetrics and Gynecology, 18*(5), 481–484.

Perona, P., & Malik, J. (1990). Scale-space and edge detection using anisotropic diffusion. Pattern analysis and machine intelligence. *IEEE Transactions On, 12*(7), 629–639.

Pohls, U. G., & Rempen, A. (1998). Fetal lung volumetry by three-dimensional ultrasound. *Ultrasound in Obstetrics and Gynecology, 11*(1), 6–12.

Rankin, R. N., Fenster, A., Downey, D. B., Munk, P. L., Levin, M. F., & Vellet, A. D. (1993). Three-dimensional sonographic reconstruction: techniques and diagnostic applications. *American Journal of Roentgenology, 161*(4), 695–702.

Roberts, L. J., Bewley, S., Mackinson, A. M., & Rodeck, C. H. (1995). First trimester fetal nuchal translucency—problems with screening the general-population. 1. *British Journal* of *Obstetrics* and *Gynaecology 102*(5), 381–385.

Rosenfield, K., Boffetti, P., Kaufman, J., Weinstein, R., Razvi, S., & Isner, J. M. (1992). 3-dimensional reconstruction of human carotid arteries from images obtained during noninvasive B-mode ultrasound examination. *American Journal of Cardiology, 70*(3), 379–384.

Salustri, A., & Roelandt, J. (1995). Ultrasonic 3-dimensional reconstruction of the heart. *Ultrasound in Medicine and Biology, 21*(3), 281–293.

Schild, R. L., Wallny, T., Fimmers, R., & Hansmann, M. (1999). Fetal lumbar spine volumetry by three-dimensional ultrasound. *Ultrasound in Obstetrics and Gynecology, 13*(5), 335–339.

Snijders, R. J. M., Noble, P., Sebire, N., Souka, A., Nicolaides, K. H., & Grp, F. M. F. F. T. S. (1998). Uk multicentre project on assessment of risk of trisomy 21 by maternal age and fetal nuchal-translucency thickness at 10–14 weeks of gestation. *Lancet, 352*(9125), 343–346.

Snijders, R. J. M., Sundberg, K., Holzgreve, W., Henry, G., & Nicolaides, K. H. (1999). Maternal age- and gestation-specific risk for trisomy 21. *Ultrasound in Obstetrics and Gynecology, 13*(3), 167–170.

Souka, A. P., Krampl, E., Bakalis, S., Heath, V., & Nicolaides, K. H. (2001). Outcome of pregnancy in chromosomally normal fetuses with increased nuchal translucency in the first trimester. *Ultrasound in Obstetrics and Gynecology, 18*(1), 9–17.

Wee L. K., Lim M., & Supriyanto, E. (2010a). Automated Risk Calculation For Trisomy 21 Based On Maternal Serum Markers Using Trivariate Lognormal Distribution. *Proceedings of the 12th WSEAS International Conference on Automatic Control, Modelling & Simulation (ACMOS 2010)*. pp. 327–332.

Taipale, P., Hiilesmaa, V., Salonen, R., & Ylostalo, P. (1997). Increased nuchal translucency as a marker for fetal chromosomal defects. *New England Journal of Medicine, 337*(23), 1654–1658.

Terris, M. K., & Stamey, T. A. (1991). Determination of prostate volume by transrectal ultrasound. *Journal of Urology, 145*(5), 984–987.

Ville (2010). Semi-automated measurement of nuchal translucency thickness: Blasphemy or oblation to quality? *Ultrasound in Obstetrics & Gynecology*. *36*(4), 400–403.

Wald, N. J., George, L., Smith, D., Densem, J. W., & Pettersonm, K. (1996). On behalf of the International Prenatal Screening Research, G. Serum Screening For Down's Syndrome Between 8 And 14 Weeks Of Pregnancy. *BJOG: An International Journal of Obstetrics & Gynaecology, 103*(5), 407–412.

Wald, N. J., Rodeck, C., Hackshaw, A. K., Walters, J., Chitty, L., Mackinson, A. M., & Group, S. R. (2003). First and second trimester antenatal screening for down's syndrome: the results of the serum, urine and ultrasound screening study (suruss). *Health Technology Assessment (Winchester, England), 7*(11), 1–77.

Wee, L. K., Miin, L., & Supriyanto, E. (2010). Automated trisomy 21 assessment based on maternal serum markers using trivariate lognormal distribution. *WSEAS Transactions on Systems, 9*(8), 844–853.

Wee, L. K., Chai, H. Y., & Supriyanto, E. (2011). Computerized nuchal translucency three dimensional reconstruction, visualization and measurement for trisomy 21 prenatal early assessment. *International Journal of Physical Sciences, 6*(19), 4640–4648.

Zosmer, N., Souter, V. L., Chan, C. S. Y., Huggon, I. C., & Nicolaides, K. H. (1999). Early diagnosis of major cardiac defects in chromosomally normal fetuses with increased nuchal translucency. *BJOG: An International Journal of Obstetrics & Gynaecology, 106*(8), 829–833.